JOURNAL OF APPLIED PHYSICS **98**, 053515 (2005)

Tailoring of high-temperature photoluminescence in InAs/GaAs bilayer quantum dot structures

Yu. I. Mazur,[a] Zh. M. Wang, G. G. Tarasov,[b] Vas. P. Kunets, and G. J. Salamo
Department of Physics, University of Arkansas, Fayetteville, Arkansas 72701

Z. Ya. Zhuchenko
Institute of Semiconductor Physics, National Academy of Sciences, Prospect Nauki 41, 03028 Kiev, Ukraine

H. Kissel
Ferdinand-Braun-Institut für Höchstfrequenztechnik, Gustav-Kirchhoff-Strasse 4, 12489 Berlin, Germany

(Received 14 February 2005; accepted 27 July 2005; published online 8 September 2005)

Temperature-dependent photoluminescence is investigated in bilayer InAs/GaAs quantum dot structures with constant InAs deposition θ_1 in the seed layer, but variable deposition θ_2 in both the second layer and the GaAs spacer layer. It is shown that interlayer coupling, leading to the formation of asymmetric quantum dot pairs, strengthens the high-temperature photoluminescence and strongly influences carrier relaxation channels. We report that radiative recombination and carrier capture efficiency by the quantum dots in the second layer can be tailored using the deposition θ_2 and the GaAs spacer thickness. © *2005 American Institute of Physics*. [DOI: 10.1063/1.2039271]

I. INTRODUCTION

The high-temperature behavior of quantum dot (QD) systems is important to understand due to the fact that a quenching of photoluminescence (PL) and a rapid redshift of the emission energy are observed with increasing temperature, both of which are harmful to QD devices.[1–4] For example, at high temperatures PL quenching in the InAs/GaAs QD system is caused by the carrier escape from QDs followed by subsequent nonradiative decay in barriers or wetting layers (WLs). In addition, while for low-density QD arrays the probability of carrier tunneling is small, in dense QD systems, carrier escape can take place due to lateral coupling between neighboring QDs.[5–10] Temperature elevation can also activate carriers into the barrier or WL due to a step-by-step transition where they are retrapped by larger QDs or captured by nonradiative centers in the vicinity of the barrier or WL.[2] Together these processes lead to a quenching of the PL at high temperatures resulting in a decrease of the PL intensity as well as a peak energy shift to lower energy.

In order to minimize high-temperature effects, QD systems with higher barriers, such as InAs/$Al_xGa_{1-x}As$, have been proposed to prevent carrier escape.[11–13] Such systems provide stronger confinement due to a larger band-gap difference at the Γ point. For example, between InAs and AlAs (~1.7 eV at low temperature) in comparison with InAs and GaAs (~1.1 eV at low temperature).[9]

Temperature effects are particularly interesting in multilayered QD structures. For example, in bilayer InAs/GaAs QD systems, PL measurements have revealed a blueshifted emission of the second QD layer with respect to the seed layer.[14] This is attributed to an enhanced intermixing during the capping stage of the second-layer QDs. The blueshift is somewhat reduced for annealed spacer layers due to a reduction in the strain in the spacer layer. Therefore, interestingly, the PL emission spectrum from the small quantum dots (SQDs) of the seed layer and the large quantum dots (LQDs) of the second layer can be made more coincident by increasing the amount of InAs deposited in the second layer or by annealing the spacer layer. Thus, there exist various factors that can affect the PL in bilayer structures. In this paper, we show that interlayer coupling is a crucial factor for high-temperature stabilization of the PL response in such a system.

II. SAMPLES AND EXPERIMENTAL DETAILS

Varying InAs coverage in the second layer θ_2, GaAs spacer layer (d_{sp}) between the seed and second layers, growth temperatures, and annealing times for each QD layer, different vertically correlated pairs of unequal sized QDs (bilayer QD structures) have been grown. Such a system is called an "asymmetric QD pair"[15] (AQDP) and is ideally suited both for the exploration of multilayered QD structures and for effective control over the uniformity of size, shape, and density of the QDs in the second layer. This latter property increases the potential of AQDPs for applications. The AQDP samples explored here were grown using a solid-source molecular-beam epitaxy chamber coupled to an ultrahigh-vacuum scanning tunneling miroscope (STM). The structures were grown on a GaAs (001) substrate, followed by a 0.5-μm GaAs buffer layer, 28-nm $Al_{0.3}Ga_{0.7}As$ layer, 57-nm GaAs layer, 1.8-ML (monolayer) InAs seed layer, variable GaAs spacer layer, variable InAs QDs layer covered by 57-nm GaAs layer, and 28-nm $Al_{0.3}Ga_{0.7}As$ layer. The total structure was capped by a 20-nm GaAs layer. Before deposition of a 1.8-ML InAs seed layer, a 10-min annealing at substrate temperature of 580 °C was used to provide a nearly defect-free atomically flat surface. The seed QD layer

[a]Electronic mail: ymazur@uark.edu
[b]On leave from Institute of Semiconductor Physics, National Academy of Sciences of Ukraine, Prospect Nauki 45, 03028 Kiev, Ukraine.

 © 2005 American Institute of Physics

Downloaded 26 Sep 2005 to 141.20.41.93. Redistribution subject to AIP license or copyright, see http://jap.aip.org/jap/copyright.jsp

TABLE I. Structural parameters of the two studied sets of samples.

	S27	S28	S29	S30	S35	S36	S37
InAs seed layer, $\theta_1(ML)$	1.8	1.8	1.8	1.8	1.8	1.8	1.8
GaAs spacer layer, $d_{sp}(ML)$	50	50	50	50	30	40	60
InAs second layer, $\theta_2(ML)$,	1.8	2.1	2.4	2.7	2.4	2.4	2.4

was grown at a growth rate of 0.1 ML/s, As_4 partial pressure of 8×10^{-6} Torr, and substrate temperature of 500 °C. The growth rate of the GaAs spacer layer was 1.0 ML/s. In this study we consider two sets of samples: (i) One with a variable GaAs spacer layer, d_{sp}, and the other (ii) with variable deposition, θ_2, of the second InAs layer. The details on these samples are shown in Table I.

Previous studies of these samples by plane-view STM and cross-sectional transmission electron microscopy (XTEM) were done.[16] The STM statistical analysis indicates a size distribution for the QDs with (4.0 ± 1.5) nm for the height in the seed layer. The dot density in the second layer is variable over the range of $(2.5-4.0)\times10^{10}$ cm^{-2} depending on the value of d_{sp}. Meanwhile, the second-layer three-dimensional (3D) islands are nearly *twice the volume* of the seed islands (for $d_{sp}=30$ ML) due to the higher deposition, as well as the influence of the strain field from the seed layer. The XTEM images show that growth results in a vertically correlated bilayer QD structure with different sized dots in each layer. However, the correlation is not complete, and a fraction of the SQDs of the seed layer as well as the LQDs of the second layer is still uncoupled. The STM statistical analysis proves, as one might expect, that the fraction of correlated QDs among the total number of QDs in the bilayer structure strongly depends on the spacer thickness d_{sp}.

The PL was studied in the temperature range of 10 −320 K using the 514.5-nm line of an Ar^+ laser for above AlGaAs barrier excitation and spanning excitation densities from 0.1 to 20 W/cm^2. A liquid-N_2-cooled Ge photodiode in conjunction with a 1.0-m double-grating monochromator was used for detection.

III. EXPERIMENTAL RESULTS AND DISCUSSION

Temperature-dependent PL measurements have been carried out for a set of bilayer samples with the deposition $\theta_1=1.8$ ML in the seed layer and $\theta_2=2.4$ ML in the second layer, but variable spacer layer thicknesses d_{sp}: $d_{sp}=30$, 40, 50, and 60 ML in the samples S35, S36, S29, and S37, respectively. The laterally varying surface stress caused by the buried InAs QDs of the seed layer favors the formation of AQDPs (Ref. 15 and 16) consisting of SQDs in the seed layer and LQDs in the second layer. While $\theta_2>\theta_1$, the additional material in the second layer is redistributed to increase the average size of the islands and the strain field associated with islands in the second layer. The low-temperature ($T=10$ K) PL spectra shown in Fig. 1 indicate the presence of two different-sized QD families by a double-peak structure. The low-energy peak is assigned to LQDs, whereas the high-energy peak is related to SQDs. A regular redshift of the low-energy peak, seen in Fig. 1 for decreasing d_{sp}, gives evidence of an enlarged QD volume in the second layer due

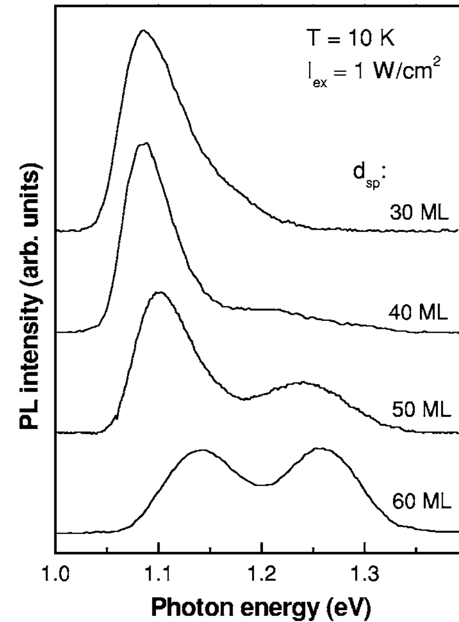

FIG. 1. Low-temperature PL spectra for a set of bilayer InAs/GaAs QD samples with a deposition $\theta_1=1.8$ ML in the seed layer and $\theta_2=2.4$ ML in the second layer, but variable spacer layer thicknesses d_{sp}: $d_{sp}=30$, 40, 50, and 60 ML in samples S35, S36, S29, and S37, respectively. The PL features corresponding to SQDs (high-energy peak) and LQDs (low-energy peak) can be clearly distinguished in each spectrum.

to correlated vertical growth. Meanwhile, a narrowing full width at half maximum (FWHM) of the low-energy PL peak with decreasing d_{sp} is attributed to an improved uniformity of the LQDs under vertical strain-driven epitaxy.[15] Interestingly, the magnitude of the broad high-energy PL feature essentially drops down if d_{sp} reaches the value of ~30 ML. Such an abrupt fading of the SQDs emission with decreasing d_{sp} is attributed to efficient carrier transfer between the SQDs and the LQDs in the AQDP system.[17] The mechanism of carrier transfer from SQDs to LQDs within the AQDP system is likely due to nonresonant tunneling. Its efficiency exponentially depends on the height of the barrier separating SQDs and LQDs. Thus, the analysis of the low-temperature PL in the investigated set of samples proves that optical emission from excitons in the AQDP is the dominant PL mechanism.

In this paper we consider the PL emission from the grown set of samples at high temperatures. We observe dramatic changes for the PL contributions from the SQDs and LQDs. Figure 2 clearly demonstrates these changes. The SQDs emission is completely quenched at room temperature and in its place we find a tail at the high-energy side of the PL from the LQDs. Meanwhile, the magnitude of the PL from the LQDs follows an inverse dependence on d_{sp} in the investigated set of bilayer samples. The most stable emission as a function of temperature occurs in sample S35 with the GaAs spacer $d_{sp}=30$ ML. In contrast, for sample S37, having the largest spacer $d_{sp}=60$ ML, the PL amplitude is completely quenched at $T=290$ K. This important finding contradicts the observation made in Ref. 2, which claims that both carrier capture and radiative efficiency of QDs are expected to drop significantly when reducing the spacer thickness.

In addition to the observed PL amplitude dependence, a

Downloaded 26 Sep 2005 to 141.20.41.93. Redistribution subject to AIP license or copyright, see http://jap.aip.org/jap/copyright.jsp

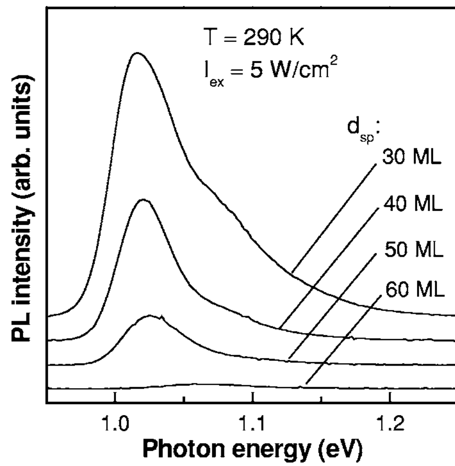

FIG. 2. High-temperature PL spectra for the same set of samples as in Fig. 1. The SQDs emission is quenched. The highest magnitude of a LQDs PL feature is detected in sample S35 with the strongest interlayer coupling.

strong redshift of the PL maximum with increasing temperature is also observed for all of the samples. Interestingly, the dependence $E_{\max}(T)$ shown in Fig. 3 cannot be fully explained if only the energy gap shrinking of $E_g^{\mathrm{GaAs}}(T)$ and/or $E_g^{\mathrm{InAs}}(T)$ or even if the temperature-induced redistribution of carriers in favor of the largest QDs of the second layer is taken into account. The $E_{\max}(T)$ dependence of sample S37 resembles the so-called "sigmoidal" temperature dependence observed in dense QD arrays ($\sim 10^{12}$ cm^{-2}) (Ref. 3 and 8) with pronounced multimodal QD size distributions. In the case of a multimodal distribution, the significant change in the $E_{\max}(T)$ slope can be attributed to different temperature dependencies of the radiative efficiency inherent to different QD families.[8] Within a single family, the $E_{\max}(T)$ dependence normally follows the Varshni's law for the temperature-dependent shift of bulk energy gaps.[18,19] At intermediate temperatures, due to lateral QD coupling, carrier transfer from the higher-energy to the lower-energy dot families takes place and consequently the LQDs families play an increasing role in the spectra. The crossover takes place around 40–50 K for a single InAs/GaAs QD layer.[8] In our system the areal density of QDs in the seed layer is low enough ($\sim 10^{10}$ cm^{-2}) preventing immediate lateral QDs coupling (through tunneling) and the LQDs density in the second layer is even lower. Therefore we could relate the sigmoidal $E_{\max}(T)$ dependence in sample S37 to the interlayer QD coupling only, resulting in an energy transfer from the seed to the second layer. The $E_{\max}(T)$ dependence in the other samples of this set shows a subsequent flattening as d_{sp} becomes smaller. The ensemble effect attributed to a preferential quenching of the PL from smaller QDs due to the smaller carrier localization energy is obviously smaller in sample S35 in comparison with sample S37. The thinner the spacer, the more the temperature evolution of the transition energy $E_{\max}(T)$ is determined by intrinsic properties of coupled QDs (AQDP). It is worth noticing that the high-temperature $E_{\max}(T)$ dependence in samples S35 and S36 follows the expected $E_g(T)$ dependence of bulk GaAs.

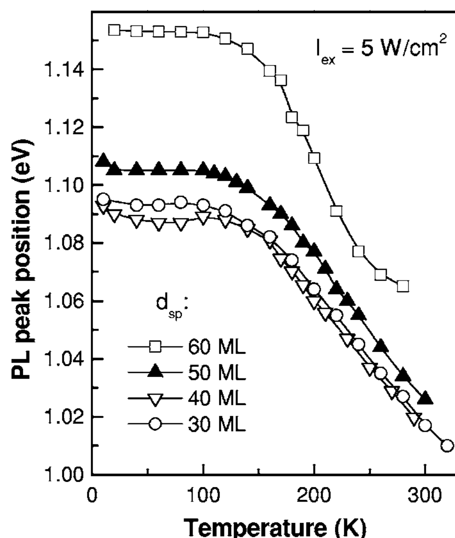

FIG. 3. Temperature dependence of the LQDs ground-state emission energy for the same set of samples as in Figs. 1 and 2. A "sigmoidal" dependence $E_{\max}(T)$ is detected for sample S37 with a thick spacer related to the different carrier relaxations in the families of coupled and noncoupled LQDs.

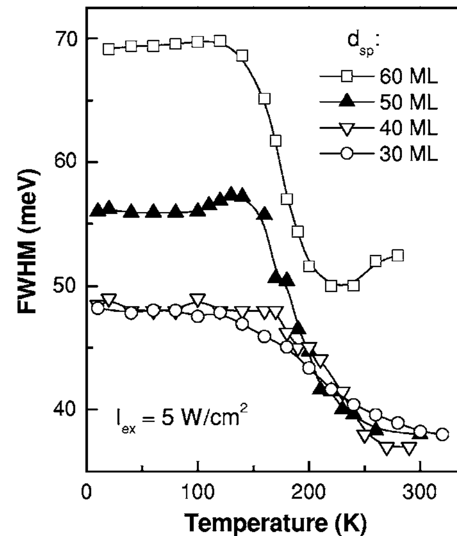

FIG. 4. Temperature dependence of the FWHM for the LQDs emission in the same set of samples as in Figs. 1–3. The reduction of the FWHM at 200 K by 30% observed in sample S37 is related to lateral carrier transfer.

The temperature evolution of the FWHM and the integrated intensity of LQDs PL for the investigated set of samples are shown in Figs. 4 and 5. We observe a correlation between the dependence of $E_{\max}(T)$ and the FWHM(T). For example, for sample S37 the onset of a steep red shift in the $E_{\max}(T)$ dependence correlates with the onset of a significant FWHM shrinkage. The decreasing FWHM in sample S37 can give evidence for thermally induced lateral energy transfer via the WL. Such a lateral coupling of QDs could enable the formation of a position-independent Fermi level at high temperatures. The FWHM decreases by $\sim 30\%$ if the temperature increases from 120 up to 200 K, reflecting preferential quenching of the PL from the smaller QDs in the second layer. Meanwhile an increase of the FWHM is observed if the temperature is elevated up to 300 K. This behavior might be attributed to an increase in the number of carriers transferred to the LQDs.

The dependence of the FWHM on temperature is found

Downloaded 26 Sep 2005 to 141.20.41.93. Redistribution subject to AIP license or copyright, see http://jap.aip.org/jap/copyright.jsp

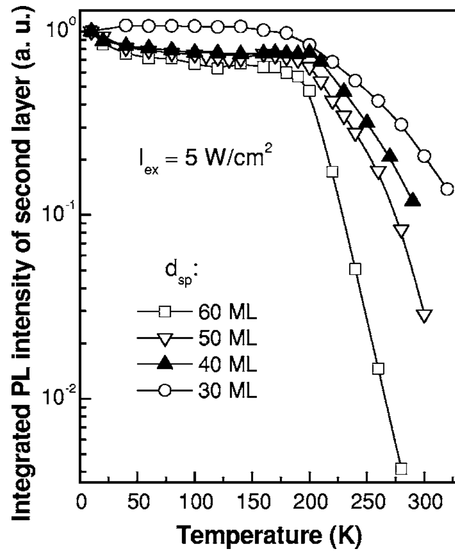

FIG. 5. Temperature dependencies of the normalized integral PL intensities $I_{int}(T)/I_{int}(10\text{ K})$, in the same set of samples as in Figs. 1–4. A rapid decay of the LQDs emission is observed in the sample S37, whereas a comparatively strong PL gain is detected from the AQDP in sample S35 with strong interlayer coupling.

to diminish with decreasing d_{sp}. Note that due to the rapid decay with temperature of a SQDs feature near the LQDs peak, the accurate determination of the FWHM of the LQDs feature is consequently more complicated at higher temperatures. The temperature dependence of the integrated PL, $I_{int}(T)$, shown in Fig. 5 demonstrates the temperature quenching rate of the LQDs PL as a function of spacer thickness d_{sp}. For this purpose each $I_{int}(T)$ is normalized with respect to its low-temperature (T=10 K) value. It is clearly seen that the decay of the LQDs emission is substantially hindered in the bilayer system with the thinnest spacer (d_{sp}=30 ML). The decay rate is found to be maximal for d_{sp}=60 ML when the QD layers are essentially weakly coupled through a thick GaAs barrier. For example, for sample S37 the integrated intensity decreases beginning from ~100 K, and the steepest part of the $I_{int}(T)$ dependence begins at ~170 K. In order to uncover the processes involved in the PL degradation with increasing temperature, we consider two thermally activated nonradiative recombination processes. The activation energies of E_1=330 meV and E_2=120 meV have been derived from a fit using Eq. (1),[18]

$$I/I_0 = \{1 + C_1 \exp(-E_1/kT) + C_2 \exp(-E_2/kT)\}^{-1}. \quad (1)$$

The first energy E_1 is close to the localization energy of the ground-state exciton with respect to the WL. However, it is more reasonable to assume that the single-carrier activation energy [while the exciton binding energy in InAs/GaAs QDs is ~10 meV (Ref. 6)] is considerably smaller than the carrier localization and quantization energies and that the escape of one carrier already quenches the PL. Additionally, a reduction of the carrier capture efficiency with increasing temperature has to quench the QD PL intensity for nonresonant excitation.[18] Meanwhile, E_2 is close to the energy difference between the ground-state emissions in LQDs and SQDs. In Ref. 18 the smaller activation energy has been ascribed to the respective excited-state splitting observed for similar bilayer systems in a high-density PL experiment. If one takes into account a much more complicated structure of the excited-state density, such a description seems to be a bit ambiguous. A further analysis of the $I_{int}(T)$ dependence shown in Fig. 5 can hardly be performed in terms of two activation energies.

Comparing the data plotted in Fig. 1 one can see a blueshift of the LQD PL feature for the case of a 60-ML thick spacer. There exist at least two origins for such shift. First is due to the change of the geometrical size of the LQDs when comparing practically uncoupled QDs layers to coupled layers. The second origin can be due to the increasing strain in the upper QD layer. Higher strain would result in higher probability for defect formation with an increasing amount of deposited material, thus explaining the rapid quenching of the PL intensity from the sample with a 60-ML thick spacer (Fig. 5) and from the sample with a 50-ML-thick spacer and with a θ_2 of 2.1 ML. However, effective defect generation is expected in the case of inhomogeneous strain rather than in the case of simply higher strain. Such inhomogeneous strain is characteristic of the strain-driven growth of a bilayer QDs system with a thinner spacer layer (e.g., 30 and 40 ML in our experiment). Thus, one could expect higher defect concentration in the system with a thinner spacer, but the fact of a temperature stabilization of the PL for smaller than 60 ML of GaAs spacer thicknesses contradicts such an assumption. Therefore the second origin should be ruled out as an explanation for the LQD PL temperature behavior observed with variation of the GaAs spacer thickness.

Taking all experimental findings into account we assume that the temperature behavior of the LQDs PL is controlled to great extent by inter layer coupling resulting in the appearance of stable AQDPs. In the case of low temperature the LQDs of the AQDP effectively accumulate carriers from the SQDs of AQDPs due to nonresonant tunneling. Likewise, the SQDs of the seed layer of the AQDP serve as the largest QDs for the energy accumulation through lateral tunneling or carrier transfer at higher temperatures. That is, the carriers that are being thermally activated into the WL or barrier can be further retrapped by QDs in the seed layer of the AQDPs. This thermally induced carrier flux enhances the high-temperature LQDs PL and therefore favors its temperature stability. Meanwhile, the complicated temperature behavior of the LQDs PL observed with increasing interlayer spacing is related to the appearance of noncorrelated LQDs in the second layer realizing a new "family" of LQDs that relaxes independently. This is the reason for the sigmoidal $E_{max}(T)$ dependence found in sample S37. According to this model the thermal step-by-step excitation of carriers into the WL or barrier continuum has to be dominated by thermal carrier transfer back from the LQDs of the second layer, to the ground state of SQDs in the seed layer, thus enhancing the high-temperature SQDs PL that is quenched at intermediate temperatures. Therefore we consider the strongly developed high-energy asymmetry of the LQDs PL feature (see Fig. 2) as a result of thermally coupled QDs ground states in the AQDP.

It is natural to assume that the PL stability depends on the AQDP geometry. For this purpose a set of bilayer

Downloaded 26 Sep 2005 to 141.20.41.93. Redistribution subject to AIP license or copyright, see http://jap.aip.org/jap/copyright.jsp

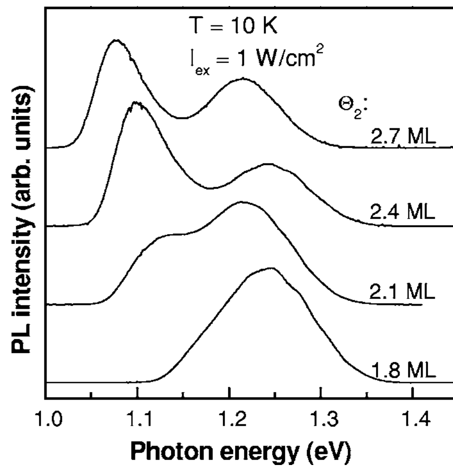

FIG. 6. Low-temperature PL for a set of bilayer samples with the deposition $\theta_1=1.8$ ML in the seed layer, a fixed spacer thickness $d_{sp}=50$ ML, and variable deposition θ_2 in the second layer: $\theta_2=1.8$, 2.1, 2.4, and 2.7 ML in samples S27, S28, S29, and S30, respectively. A single-peak spectrum is detected for sample S27 with $\theta_1=\theta_2$.

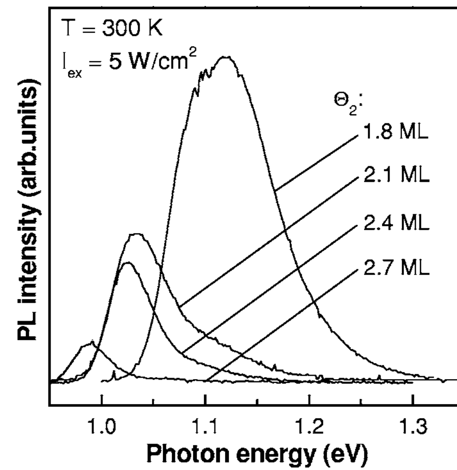

FIG. 7. High-temperature PL spectra for the same set of samples as in Fig. 6. The SQDs emission is quenched. The highest magnitude of LQDs PL feature is detected in sample S27 with $\theta_1=\theta_2$. The high-energy asymmetry of the LQDs PL feature is related to thermal re-excitation of the SQDs and thermal population of the excited states of LQDs of the second layer.

samples with the deposition $\theta_1=1.8$ ML in the seed layer, fixed spacer thickness $d_{sp}=50$ ML, and variable deposition θ_2 in the second layer: $\theta_2=1.8$, 2.1, 2.4, and 2.7 ML in samples S27, S28, S29, and S30, respectively, was prepared. Due to the comparatively thick spacer the growth results in a partially vertically correlated bilayer QD structure with available AQDP. The STM statistical analysis shows that the fraction of correlated QDs among the total QD number in the bilayer structure is 50%. The QDs in the second layer gradually enlarge with increasing deposition θ_2. That means the QDs detuning θ_2 in the AQDP grow at the same interlayer electronic coupling. Figure 6 shows the low-temperature ($T=10$ K) PL spectra for this set of samples. The spectra transform from an unresolved broad spectral feature at 1.233 eV in the case of $\theta_1=\theta_2$ into a double-peak spectrum for sample S30. The LQDs PL feature shifts regularly to the red side of the spectrum from 1.233 eV in sample S27 to 1.065 eV in sample S30. The FWHM reaches a value of ~54 meV in sample S30 indicating a narrow QD size distribution.

The high-temperature PL spectra of this set of samples are shown in Fig. 7. The LQDs PL quenches most rapidly in sample S30 with the largest QDs, while the PL gain of sample S27 is the most stable. This tendency is reproduced in Fig. 8, where each $I_{int}(T)$ dependence is normalized with respect to its low-temperature ($T=10$ K) value. One can see that the decay of the LQDs emission is substantially hindered in the bilayer system with equal depositions, $\theta_1=\theta_2$. At first sight this tendency appears to contradict what was observed in the first set of samples with varying spacer thickness. Indeed, it has been discovered that by decreasing the spacer thickness larger QDs in the AQDP have been produced, thus stabilizing the PL yield. In the second set the increase of the QD sizes results in lower stability of the PL. In fact, both tendencies are consistent. Indeed, the contribution of the AQDP in the broad PL spectrum of sample S27 is not spectrally resolved. Nevertheless, such pairs can be distinctly resolved in the samples with larger θ_2. With increasing temperature the noncoupled QD emission rapidly decays in both layers and only the emission from the AQDP survives. The unusually large redshift of the LQDs PL observed in sample S27 with increasing temperature from 20 to 300 K supports this assumption. Indeed, it reaches a value of ~130 meV in sample S27 in comparison with ~75 meV observed in other samples of this series. The temperature dependencies of $E_{max}(T)$ and FWHM (T) for sample S27 are also consistent with such an assumption, demonstrating a pronounced sigmoidal behavior for the energy of the ground-state emission and the deep minimum at $T=200$ K in the FWHM (T) dependencies. A comparison of the high-temperature PL results gives evidence that the PL stability is unambiguously determined by the competition between intradot relaxation and competing processes such as thermally induced escape and interdot transfer of carriers within the AQDP. This latter being of crucial importance is determined by interlayer electronic coupling that in turn depends on the spacer thickness, strain topology, and the QD sizes. By optimizing various

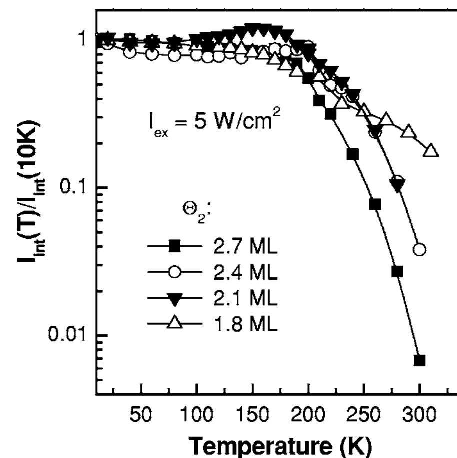

FIG. 8. The temperature dependencies of the normalized integral PL intensities $I_{int}(T)/I_{int}(10\text{ K})$ in the same set of samples as in Figs. 6 and 7. A rapid decay of the LQDs emission is observed in sample S30 with the largest QDs in the second layer, whereas a more stable PL yield is detected from the AQDP in sample S27.

Downloaded 26 Sep 2005 to 141.20.41.93. Redistribution subject to AIP license or copyright, see http://jap.aip.org/jap/copyright.jsp

factors it is possible to realize a QD structure of molecular type, asymmetric QD pairs with their own intramolecule carrier relaxation determining the PL stability.

IV. CONCLUSIONS

We have investigated the temperature dependence of the PL from a bilayer InAs/GaAs QDs structure with constant InAs deposition θ_1 in the seed layer, but variable deposition θ_2 in the second layer and a GaAs spacer layer thickness. It is shown that interlayer coupling leading to the formation of asymmetric quantum dot pairs strengthens the high-temperature PL and strongly influences carrier relaxation channels. Further, results show that the stable radiative recombination and capture efficiency of the QDs in the second layer can be tailored through a compromise between the deposition θ_2 and the spacer thickness. It is clear that to optimize the AQDP structure it is important to provide an optimization of the whole bilayer structure by means of (i) preventing intermixing during the capping process of the second layer of QDs for increased strain-relaxed QDs, (ii) avoiding a deterioration of the GaAs barrier with decreasing interlayer spacing caused by the accumulation of nonradiative centers in the GaAs barrier, and (iii) tuning the WL states in order to space them out from the QD ground states. This can be reached by an increase of the barrier band gap taking into account the different wave-function penetrations of the WL and QD states in the barrier or additionally confining the bilayer structure with AlGaAs barriers thus preventing the carrier escape out of the bilayer volume. All of these factors should be taken into account when fabricating bilayer QD samples for optical device applications.

ACKNOWLEDGMENTS

The authors acknowledge the financial support of the National Science Foundation of US (through Grant Nos. PHY-0099496 and DMR-0080054) and Ukrainian State Foundation for Fundamental Researches.

[1] D. Bimberg, M. Grundman, and N. N. Ledentsov, *Quantum Dot Heterostructures* (Wiley, Chichester, 1999).
[2] S. Sanguinetti, M. Padovani, M. Gurioli, M. Guzzi, A. Vinattieri, M. Colocci, P. Frigeri, and S. Franchi, Appl. Phys. Lett. **77**, 1307 (2000).
[3] G. G. Tarasov, Yu. I. Mazur, Z. Ya. Zhuchenko, A. Massdorf, D. Nickel, J. W. Tomm, H. Kissel, C. Walter, and W. T. Masselink, J. Appl. Phys. **88**, 7162 (2000).
[4] E. C. Le Ru, J. Fack, and R. Murray, Phys. Rev. B **67**, 245318 (2003).
[5] D. Colombo, S. Sanguinetti, E. Grilli, M. Guzzi, L. Martinelli, M. Gurioli, P. Frigeri, G. Trevisi, and S. Franchi, J. Appl. Phys. **94**, 6513 (2003).
[6] D. I. Lubyshev, P. P. González-Borrero, E. Marega, Jr., E. Petitprez, N. La Scala Jr., and P. Basmaji, Appl. Phys. Lett. **68**, 205 (1996).
[7] Z. Y. Xu *et al.*, Phys. Rev. B **54**, 11528 (1996).
[8] L. Brusaferri *et al.*, Appl. Phys. Lett. **69**, 3354 (1996).
[9] Z. Ma, K. Pierz, and P. Hinze, Appl. Phys. Lett. **79**, 2564 (2001).
[10] J. W. Tomm, T. Elsaesser, Yu. I. Mazur, H. Kissel, G. G. Tarasov, Z. Ya. Zhuchenko, and W. T. Masselink, Phys. Rev. B **67**, 045326 (2003).
[11] S. Fafard *et al.*, Surf. Sci. **361/362**, 778 (1996).
[12] H. Y. Liu *et al.*, J. Cryst. Growth **210**, 451 (2000).
[13] A. Polimeni, A. Patane, M. Henini, L. Eaves, and P. C. Main, Phys. Rev. B **59**, 5064 (1999).
[14] P. B. Joyce, E. C. Le Ru, T. J. Krzyzewski, G. R. Bell, R. Murray, and T. S. Jones, Phys. Rev. B **66**, 075316 (2002).
[15] R. Heitz, I. Mukhametzhanov, J. Zeng, P. Chen, A. Madhukar, and D. Bimberg, Superlattices Microstruct. **25**, 97 (1999).
[16] Yu. I. Mazur, Z. M. Wang, G. J. Salamo, M. Xiao, G. G. Tarasov, Z. Ya. Zhuchenko, W. T. Masselink, and H. Kissel, Appl. Phys. Lett. **83**, 1866 (2003).
[17] R. Heitz, A. Kalburge, Q. Xie, M. Grundmann, P. Chen, A. Hoffmann, A. Madhukar, and D. Bimberg, Phys. Rev. B **57**, 9050 (1998).
[18] R. Heitz, I. Mukhametzhanov, A. Madhukar, A. Hoffmann, and D. Bimberg, J. Electron. Mater. **28**, 520 (1999).
[19] Y. P. Varshni, Physica (Utrecht) **34**, 149 (1967).

Downloaded 26 Sep 2005 to 141.20.41.93. Redistribution subject to AIP license or copyright, see http://jap.aip.org/jap/copyright.jsp